Max-Planck-Institut
für Meteorologie

REPORT No. 25

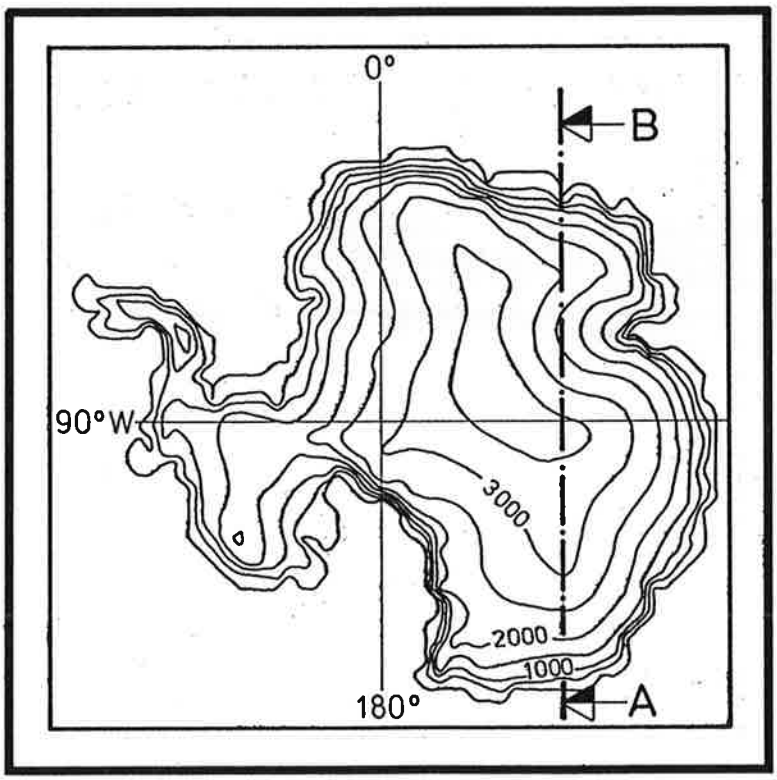

A THREE-DIMENSIONAL ICE-SHEET MODEL: TEST CASE ANTARCTICA

by

KLAUS HERTERICH

HAMBURG, JANUARY 1989

AUTHOR:

KLAUS HERTERICH

MAX-PLANCK-INSTITUT
FUER METEOROLOGIE

MAX-PLANCK-INSTITUT
FUER METEOROLOGIE
BUNDESSTRASSE 55
D-2000 HAMBURG 13
F.R. GERMANY

Tel.: (040) 4 11 73-0
Telex: 211092
Telemail: MPI.Meteorology
Telefax: (040) 4 11 73-298

A three-dimensional ice-sheet model: test case Antarctica

by
Klaus Herterich
Max-Planck-Institut für Meteorologie
Bundesstr. 55,
2000 Hamburg 13, FRG

Abstract

A preliminary version of a three-dimensional ice-sheet model for later use in climate models, still excluding ice-shelf, is presented and applied to the Antarctic-Ice-Sheet. In the model, the 3-d fields of velocity and temperature are calculated in the coupled mode and the temperature equation is integrated for 50 000 years, with the shape of the Antarctic-Ice-Sheet kept fixed. The model results are consistent with a stationary state in the central parts of the Antarctic-Ice-Sheet but not in marginal areas, where the model-ice flow is too small. Including a parameterized form of basal sliding, depending on the water pressure, is likely to improve the situation.

1.Introduction

Modeling climatic change on time scales longer than 100 years has to consider the dynamics of ice-sheets, which in turn alter the boundary conditions of the other components of the climatic system. During the last 20 years, data of the long term variations in the global ice volume and of many other climate variables have been derived from deep-sea sediment records (sea-surface temperature, carbon cycle) and from sediments on land (temperature, humidity). Thus many ice-sheet models, including the coupling to models of the atmosphere, the ocean, and the continent have been developed to study climate dynamics on time scales ranging from 10^3 to 10^6 years.

The hierarchy of ice-sheet models includes simple models as well as complex circulation models. Simple 1-d ice-sheet models were introduced by Weertman (1976). Such models provided a first insight into the dynamics of ice-sheets. The most sophisticated ice-sheet model was developed by Jenssen (1977) to describe the Greenland-Ice-Sheet. In his model, the 3-dimensional velocity and temperature field is calculated. Starting from present conditions, the evolution of the

ice-sheet was modelled for several thousand years. However, predicted changes of the shape of the Greenland-Ice-Sheet could have several interpretations. Either the Greenland-Ice-Sheet is not in a stationary state now, or inevitable model errors were the cause of the observed drift.In a numerical simulation for the Antarctic-Ice-Sheet, Oerlemans (1982) demonstrated the principal usefulness of a 3-d ice-sheet model to describe at least the gross features of ice-sheet dynamics. He used a vertically integrated description and was able to build up the Antarctic-Ice-Sheet by coupling to a simple model of the atmosphere, which specified the mass balance (snow fall and ice melt).

Nevertheless, there is still some debate on the usefulness of high resolution descriptions of ice-sheets concerning climate change. Saltzman (1984) pointed out that small errors in the mass balance will ultimately drive the model-ice-sheet to a quite different state compared to that one actually chosen by nature, using the real mass balance. Thus the predictive skill would decrease with the length of the integration time. He suggests the use of simpler models with some free parameters, which can be tuned in such a way, to obtain a good fit between the model and the data.However, there are also good reasons to use complex ice-sheet models of the Jenssen type to predict the evolution of the ice-sheet, provided the time integration is not extended too far. Within the range of these shorter intervals are investigations of the stability of ice-sheets as for example the stability of the West-Antarctic-Ice-Sheet. Meaningful shorter interval integrations may be performed also with the (ice-age) ice-sheets of the Northern-Hemisphere, concerning their initial build-up starting 120 000 years back in time, or modeling ice-sheet decay, with initial conditions set by 18 000 year B.P. data (CLIMAP, 1976). In all these cases, the initial conditions and the mass balance can probably be specified more precisely.

For climate studies, the most relevant ice-sheet variable, feeding back into the climate system, is the ice thickness as a function of geographical position and time (Oerlemans and van der Veen, 1984). Although a high spatial resolution is prefered, it may not be necessary to calculate the ice flow with an equally high precission, provided integration times are not too long (100 000 years say). Due to the non-linear relation between ice-sheet shape and ice flow, errors in the flow calculations influence the evolution of the shape of the ice-sheet only weakly, yielding changes in ice-sheet thicknesses, which may be sufficiently precise to meet climate modeling requirements. In the initial build-up phase of

the ice-sheet, basal sliding may even be neglected since the small geothermal heat flux can warm up the ice bottom only slowly.

In this paper an attempt is therefore made to pick up Jenssens idea once more and to construct a high resolution ice-sheet model. The present version does not yet contain an adequate description of basal sliding and makes no attempt to model ice-shelf. Ice-shelf is planned to be included at a later stage by coupling this ice-sheet model to the ice-shelf model of MacAyeal and Thomas (1982). In section 2, the equations, approximations, and boundary conditions are described. Preliminary results, showing the (stationary state) velocity and temperature field for the Antarctic-Ice-Sheet are presented in section 3 and discussed in section 4.

2. Model description

2.1. Equations for the velocity field

In deriving the velocity field, we start from the general set of dynamic equations for plastic ice flow, the force balance:

$$\nabla \cdot \boldsymbol{\sigma} + \rho \mathbf{g} = 0 , \tag{1}$$

and the empirical flow law:

$$\dot{\varepsilon}_{ik} = A(T') \sigma^{n-1} \sigma'_{ik} . \tag{2}$$

A derivation of eq. (1) and (2) may be found in the textbook by Paterson (1981). In eq. (1), ρ = 1 g cm^{-3} is the density of ice taken as constant, $\mathbf{g}$ the vector of Earth's acceleration ($|\mathbf{g}|$ = 9.8 m s^{-2}) and $\boldsymbol{\sigma}$ the stress tensor. Eq. (2) relates the rate of change of the components of the deformation tensor ε_{ik} with the components of the stress-deviator tensor σ'_{ik} defined by:

$$\sigma'_{ik} = \sigma_{ii} - \frac{1}{3}(\sigma_{xx} + \sigma_{yy} + \sigma_{zz}) \quad , for\ i = k , \tag{3}$$

$$and \quad \sigma'_{ik} = \sigma_{ik} , otherwise ,$$

where i, κ denote the directions of a Cartesian coordinate system with x, y the horizontal axes and z directed vertically upwards (see Fig. 1). A non-linearity enters through the second invariant σ raised to the power n-1, where n = 3 and the invariant σ defined by:

$$2\sigma^2 = \sigma'^2_{xx} + \sigma'^2_{yy} + \sigma'^2_{zz} + 2(\sigma^2_{xy} + \sigma^2_{xz} + \sigma^2_{yz}). \tag{4}$$

The temperature dependent coefficient A(T'), with T' measured relative to pressure melting point, is based on measurements compiled by Paterson (1981).

Since the rate of change of deformation can be expressed in terms of velocity gradients:

$$\dot{\varepsilon}_{i\kappa} = \frac{1}{2}\left(\frac{\partial u_i}{\partial x_k} + \frac{\partial u_k}{\partial x_i}\right), \tag{5}$$

the set of 9 equations (1), (2) can be solved in principle for the 9 unknowns, the three velocity components u_x, u_y, u_z and the six components of the (symmetric) stress tensor $\boldsymbol{\sigma}$.

For the case of an ice-sheet, following Mahaffy (1976), some approximations are introduced: In the force balance (1), the shear stresses $\sigma_{i\kappa}$ are small compared to the normal pressure σ_{ii}, which is assumed to be isotropic ($\sigma_{xx} = \sigma_{yy} = \sigma_{zz}$). The small aspect ratio of an ice-sheet (thickness small compared to horizontal extension) implies that the horizontal derivative of any (larger scale) ice-sheet variable is small compared to its vertical derivative. This (essentially) is the "shallow ice approximation" described by Hutter (1983). It can be derived formally by expanding the set (1), (2) to zero order with respect to the aspect ratio as the expansion parameter. The force balance (1) then reduces to:

$$\frac{\partial \sigma_{zz}}{\partial x} + \frac{\partial \sigma_{xz}}{\partial z} = 0,$$

$$\frac{\partial \sigma_{zz}}{\partial y} + \frac{\partial \sigma_{yz}}{\partial z} = 0, \tag{6}$$

$$\frac{\partial \sigma_{zz}}{\partial z} - \rho g = 0 .$$

The set (6) can be integrated easily to obtain the remaining three stress components:

$$\sigma_{zz} = -\rho g (h_s - z) ,$$

$$\sigma_{xz} = -\rho g (h_s - z) \frac{\partial h_s}{\partial x} , \tag{7}$$

$$\sigma_{yz} = -\rho g (h_s - z) \frac{\partial h_s}{\partial y} .$$

At the surface of the ice-sheet ($z = h_S$), the shear stresses are assumed to be zero and the atmospheric pressure has been neglected. In the approximation of a small aspect ratio, the set (5) can be inverted, thus expressing the velocity gradients as a function of the rate of change of deformation:

$$\frac{\partial u_x}{\partial z} = 2 \dot{\varepsilon}_{xz} ,$$

$$\tag{8}$$

$$\frac{\partial u_y}{\partial z} = 2 \dot{\varepsilon}_{yz} .$$

Using eqs. (2), (3), (4) and inserting the stresses (7), the set (8) can be integrated directly, yielding the two horizontal velocity components as a function of the vertical coordinate z:

$$u_x = u_x^{(B)} + C \frac{\partial h_s}{\partial x} ,$$

$$\tag{9}$$

$$u_y = u_y^{(B)} + C \frac{\partial h_s}{\partial y} ,$$

with

$$C = -2 (\rho g)^n \left[\left(\frac{\partial h_s}{\partial x} \right)^2 + \left(\frac{\partial h_s}{\partial y} \right)^2 \right]^{\frac{n-1}{2}} \int_{h_B}^{z} A (T(z')) (h_s - z')^n \, dz' . \tag{10}$$

In (9), $u_x^{(B)}$ and $u_y^{(B)}$ are the horizontal components of the basal sliding velocity and in (10), $z' = h_B$ is the height of the ice bottom (the bedrock topography). The vertical velocity component u_z follows from the incompressibility condition $\nabla \cdot \mathbf{u} = 0$:

$$u_z = u_z^{(B)} - \int_{h_B}^{z} \left(\frac{\partial u_x}{\partial x} + \frac{\partial u_y}{\partial y} \right) dz' , \tag{11}$$

with $u_z^{(B)}$, the vertical component of the basal sliding velocity.

In Mahaffy's (1976) work, the coefficient A(T') was assumed to be constant. Thus the integral in eq. (11) could be solved analytically. Further integration of (11) with respect to z yields the vertically integrated ice flux, actually calculated in her model to describe the evolution of the Barnes-Ice-Cap. A vertically integrated form was applied also by Oerlemans (1982), to build up the Antarctic-Ice-Sheet including a simple (quasi stationary) description of ice-shelfs. In Jenssen's (1977) approach, an empirical relation between the horizontal ice-velocity component and the calculated shear stresses (instead of the flow law (2)) was used, however, also temperature dependent. Furthermore, a "σ - coordinate" scheme with a variable grid size in the vertical was chosen. Although this allows a finer vertical resolution at the ice-sheet edge, it was not used in this work, since at the ice-sheet edge, the "shallow ice approximation" breaks down anyway, and numerical errors due to a coarse horizontal resolution still exist.

2.2. Temperature equation

The rate of change of temperature T within the ice-sheet is given by the energy-balance equation (for discussion see also the textbook of Paterson (1981)):

$$\frac{\partial T}{\partial t} + \mathbf{u} \cdot \nabla T = k \nabla^2 T + d . \tag{12}$$

Even in the approximation of a small aspect ratio, all three velocity components contribute to the advection term:

$$\mathbf{u} \cdot \nabla T = u_x \frac{\partial T}{\partial x} + u_y \frac{\partial T}{\partial y} + u_z \frac{\partial T}{\partial z} .$$

Although u_z is small compared to u_x and u_y, $\partial T/\partial z$ is large compared to both $\partial T/\partial x$ and $\partial T/\partial y$.

The diffusion term:

$$k\nabla^2 T = k\left(\frac{\partial^2 T}{\partial x^2} + \frac{\partial^2 T}{\partial y^2} + \frac{\partial^2 T}{\partial z^2}\right),$$

can be approximated by $k\,\partial^2 T/\partial z^2$ in most areas, but below ice divides, where horizontal advection is small, horizontal diffusion cannot be neglected.

In general, the production of deformational heat d is given by

$$d = \frac{1}{\rho c}\sum_{i,\kappa} \dot{\varepsilon}_{i\kappa}\,\sigma_{i\kappa} = \frac{1}{\rho c}\sum_{i} \dot{\varepsilon}_{ii}\,(p + \sigma'_{ii}) + \frac{1}{\rho c}\sum_{i \neq \kappa} \dot{\varepsilon}_{i\kappa}\,\sigma_{i\kappa}, \qquad (13)$$

where $p = 1/3\,(\sigma_{xx} + \sigma_{yy} + \sigma_{zz})$ is the mean (isotropic) pressure. From the incompressibility condition we have:

$$p\sum_{i} \dot{\varepsilon}_{ii} = p\sum_{i} \frac{\partial u_i}{\partial x_i} = 0\ .$$

In the "shallow ice approximation",the sum (13) is reduced further to:

$$d \approx \frac{1}{\rho c}\sum_{i \neq \kappa} \dot{\varepsilon}_{i\kappa}\,\sigma_{i\kappa} \approx \frac{2}{\rho c}\,(\dot{\varepsilon}_{xz}\,\sigma_{xz} + \dot{\varepsilon}_{yz}\,\sigma_{yz}).$$

At the ice / bedrock boundary, the geothermal heat flux G enters the ice. For temperatures below freezing point, this fixes the vertical temperature gradient at the ice bottom:

$$\left.\frac{\partial T}{\partial z}\right|_B = -\frac{G}{\lambda}, \qquad (14)$$

where $\lambda = 2.1\ W\,m^{-1}K^{-1}$ is the thermal conductivity of ice and $G = 5 \cdot 10^{-2}\ W\,m^{-2}$. If the bottom temperature reaches the melting temperature T_M, $T = T_M$ replaces

the boundary condition (14) and the geothermal heat flux is used for melting. The melting temperature is corrected for pressure:

$$T_M = -a\,\rho\,g\,h\,,$$

with h the thickness of the ice-sheet and a = $7.4 \cdot 10^{-5}$K $(kPa)^{-1}$.

At the ice / atmosphere boundary, the surface temperature T_S is prescribed. For the preliminary calculations described in section 3, a temperature of T_{SL} = -7°C was chosen at sea level, with an atmospheric lapse rate of γ = 13°C km^{-1}, taken from data (Budd et al., 1971). This defines the surface temperature for a given height h_s of the ice surface above sea level:

$$T_S = T_{SL} - \gamma h_s\,.$$

2.3. Numerical sceme

Eqs. (9), (10) and (11) for the ice flow and eq. (12) for the temperature evolution are discretized using centered differences defined on a staggered grid (Fig. 1). The temperature is defined on grid points (i, j, k), which mark the centres of volume elements $\Delta V = \Delta x \Delta y \Delta z$, for which the energy balance (12) is formulated. For calculating the advective input and output heat fluxes, it is convenient to define the normal components of the ice flow at the centers ($i \pm 1/2, j \pm 1/2, \kappa \pm 1/2$) of the 6 planes of the volume element ΔV (staggered grid).

The resolution of the grid is $\Delta x = \Delta y$ = 101 km in the horizontal and Δz = 285 m in the vertical and the time step is Δt = 10 years. To suppress numerical instabilities in the temperature equation (12), an "upstream scheme" is used, which introduces some artificial diffusion. Integration time was 50 000 years until an almost stationary temperature distribution was reached.

The numerical calculations run on a Cyber 205 (CDC) computer. Using the above resolution, computing time is 15 minutes for 10 000 model years of the Antarctic-Ice-Sheet.

2.4. Input data

All calculations that will be shown in section 3, describe an almost sationary state of the model ice-sheet. The assumed stationary shape of the Antarctic-Ice-Sheet has been derived by digitizing the maps of Drewry (1983). The resulting fields for the heights of the ice-sheet h_S, the heights of the ice bottom h_B (both measured above sea level) and the thicknesses h are shown in Figs. 2, 3 and 4 respectively.

Ice-sheet heights and thicknesses were smoothed by integrating the mass balance for 1000 years:

$$\frac{\partial h}{\partial t} = -\nabla \cdot \mathbf{q} + b \ , \tag{15}$$

where

$$\mathbf{q} = \int_{h_B}^{h_s} \mathbf{u}\, dz$$

is the vertically integrated ice flux and b the accumulation rate (taking b = 0 for smoothing purposes). Calculations showed (see section 3.1 and Fig. 6a) that small errors in the ice-surface gradient produce large errors in the vertical velocity component u_z (note that u_z involves the second deriviative of the surface height). By integrating (15) for 1000 years, the small scale variations in the sign of u_z vanish, however, larger scale variations are still recovered (Fig. 6b). The resulting new topography (thick line of Fig. 2) is about the same as in the unsmoothed case (thin line). The errors introduced by smoothing, are within the range of errors produced by digitizing the maps. During the integration of the temperature equation, the (smoothed) shape will be kept fixed. The actual surface temperature, taken as the boundary condition at the ice-sheet surface and using the parameterization of section 2.2, is plotted in Fig. 5.

3. Results

3.1. Vertical structure of velocity and temperature

In Fig. 6c, the velocity and temperature field is plotted for a vertical plane indicated by the line A-B in Fig. 7, after integrating the heat equation (12) for 50 000 years, using present day boundary conditions of the Antarctic-Ice-Sheet (section 2.4). The ice velocity is monotonically increasing from the bottom of the ice to the surface. Most of the increase with height occurs within the lower half, while the ice velocity is almost constant within the upper half.

The temperature is monotonically increasing from the surface (where the temperature is fixed) down to the bottom, reaching temperatures near or at the pressure melting point in wide areas, due to the geothermal heat input from below. The temperature gradients at the surface are generally smaller compared to bottom gradients. At places where the velocity is small, the temperature gradient within the ice is almost constant, as is expected for a stationary state if heat conduction is the only mechanism which distributes energy. Since the bottom of the ice is near the pressure melting point, the isotherms within the ice follow the bottom topography to some extent.

Velocity and temperature are coupled, since velocity depends on temperature via eqs. (9) and (10), and temperature depends on velocity due to heat transport by advection. In Fig. 6b, the velocity and temperature field for the uncoupled case is shown, taking a constant temperature of -10° C for the velocity calculations. Although the general structure of both velocity and temperature are similar with and without coupling (compare Fig. 6b and c), the absolute magnitude of the velocity is considerably smaller (by a factor 5) in the uncoupled case. Differences occur also in the absolute values of the temperature. This demonstrates the need for an accurate calculation of the ice temperature.

3.2. Vertically integrated ice flux

Fig. 7 shows the vertically integrated ice flux of an almost stationary state, reached after integrating the temperature equation (12) for 50 000 model years. The calculated flow is perpendicular to the isolines of the surface height h_s (directed downslope) and generally increases from the center towards the

margin of the ice-sheet. However, near the margin it decreases again, in contrast to observations. Calculations by Budd et al. (1971), who used the observed accumulation rate to derive the ice flux needed for a stationary state of the Antaractic-Ice-Sheet, also show an increasing ice flux downstream.

The failure of the model near the margin can be attributed to two effects: Firstly, for these calculations, the basal sliding velocity was zero, which is expected to contribute to the mass flux. Secondly, due to a coarse horizontal grid spacing, the (numerically determined) gradient of the surface topography which drives the ice flow will be underestimated at the very rim of the ice-sheet. The latter effect can be accounted for by increasing the resolution near the margin, or likewise, using a special extrapolation from the interior of the ice-sheet to estimate the correct gradient at the margin.

A more detailed evaluation of the model-ice flow is obtained by calculating the divergence of the vertically integrated flow $\nabla \cdot \mathbf{q}$, which should be equal to the observed accumulation rate b (eq. 15), provided the Antarctic-Ice-Sheet is in equilibrium to day. In Fig. 8, the observed accumulation taken from Budd et al. (1971) is shown, and compared to the model (stationary state) accumulation (Fig. 9). In the interior of the ice-sheet, the magnitude of the model accumulation (5 cm a^{-1}) is near to the observations, being positive everywhere, with increasing values downstream. However, in the model, some areas have a negative mass balance. These areas are those, which can be identified as convergence areas of the vertically integrated mass flux already by visual inspection (Fig. 7) and are probably due to the neglection of basal sliding. The negative values of the mass balance at the very rim of the Antarctic-Ice-Sheet may be in part attributed to underestimating the surface gradient there, as already pointed out above.

3.3. Bottom temperature

The importance of an accurate temperature calculation has already been demonstrated in section 3.1 showing the strong dependence of the deformational velocities on the vertical structure of the temperature field. The resulting bottom temperature is of special interest, since it probably controls the occurrence of basal sliding, which can contribute considerably to the ice flux. Only small changes in the bottom temperature decide whether there is melting at the bottom or whether the ice is frozen to the bedrock.

The bottom temperature is shown in Fig. 10. Areas where the ice is frozen to the bedrock (shaded areas) generally coincide with regions where the height of the ice bottom is above 0.5 km (see Fig. 3), thus being influenced by the cold atmosphere. Exceptions especially occur in East-Antarctica in regions of strong divergence of the vertically integrated ice flux, where, due to advection of cold ice from above, the ice bottom is frozen to the bedrock even for bottom heights below 0.5 km.

In regions of ice flux convergence (shaded areas of Fig. 9) relatively warm ice is advected from the sides, keeping the temperature at the pressure melting point. In central areas, where the flow field seems to be near to the observations (section 3.2), we also expect the bottom temperature to be correct. Indeed, the location of sub-ice lakes, as observed by Oswald and Robin (1973), coincide with areas where meltwater can be produced in the model. On the other hand, in regions where we believe that the ice flow is wrong (areas of mass-flux convergence of Fig. 9), the model bottom temperature is at the pressure melting point which opens the possibility to correct the ice flow by adding some parameterized form of basal sliding. Parameters may be the bottom temperature and the meltwater production, which can be calculated by the ice-sheet model.

3.4. Basal sliding experiments

Only two experiments have been performed using some parameterized form of basal sliding. Budd et al. (1979) suggest the sliding law:

$$u_B = c \frac{\sigma_B^m}{Z^n} , \qquad (16)$$

where σ_B is the shear stress at the ice bottom, Z a reduced ice thickness, n, m integer exponents, and c a constant.

Using eq. (16), the stationary state calculations have been repeated, inserting the real ice thickness h instead of Z, with $n = 2$, $m = 1$ and $c = 5 \times 10^4 (KPa)^{-1} m^3 a^{-1}$. The resulting fields of flow and temperature were almost identical to those without basal sliding. Provided the form (16) is to be retained, the reduced thickness Z needs to be considerably smaller than the real ice thickness (at least locally), if any effect on the flow should be visible. The physical interpretation of using a reduced thickness Z is that basal sliding should depend on the basal

pressure. In cases of melting, with water pressures of the order of the normal pressure ρgh from the weight of the ice above, basal friction may be largely reduced leading to high sliding velocities.

Since the present state of the model makes no attempt to model the flow of bottom water (from which the water pressure and thus a reduced thickness may be predicted), the constant c was increased by a factor 10, to see the effect of a sliding law of the form (16). The resulting fields of the vertically integrated ice flux, divergence of the flux, and basal temperature are plotted in Figs. 11, 12 and 13 respectively. Comparing Fig. 7 and 11 shows that the flow is now dominated by sliding with ever increasing flux downstream to the margin of the Antarctic-Ice-Sheet. The areas of negative mass balance could be reduced to some extend (compare Figs. 9 and 12). Positive mass balance of the right order of magnitude (50 cm a^{-1}) could be achieved at some places at the margin of Antarctica. Finally, the coincidence of the remaining areas of negative mass balances with areas, where the ice bottom is at the pressure melting point, is still present (compare Figs. 12 and 13). This means that there is still the possibility of improving the model by using a sliding law of the form (16), where the reduced height Z is determined by adding some law for the basal water flow. Areas of sources and sinks for the water can be obtained directly from the ice-sheet model.

4. Summary and conclusion

In this paper a preliminary version of a three-dimensional model for the Antarctic-Ice-Sheet is presented, which includes the fully coupled fields of velocity and temperature. The model does not yet contain an adequate description of basal sliding and excludes the ice-shelf regions. The results shown, are for an almost stationary state of the model, reached after 50 000 years. The stationary calculations could not prove the applicability of the model to describe the long term prognostic evolution of the Antarctic-Ice-Sheet. However, a lower limit for the necessary degree of complexity can be given for any ice-sheet model to be adequate for realistic simulations.

1. For calculations, starting with some initial conditions, the ice-surface topography has to be known quite accurately. Otherwise the vertical velocity component will have large errors, at least within the first 1000 years of integration time. For longer time integrations, the initial disturbances will

damp out, however, then the precission of the mass balance needs to be high.

2. The model should include the temperature dependence of the ice flow. This is already clear from the flow law (2), where the temperature dependent factor A(T') varies by two orders of magnitude within a temperature range from -30°C to 0°C. These temperature variations already occur within the lower half of the ice-sheet, where also most of the change of velocity with height takes place. Only those calculations, taking into account the vertical structure of temperature, yield an accumulation rate of about 5 cm a^{-1}, needed for a stationary state, which is of the order of the observed accumulation rate in the interior of the Antarctic-Ice-Sheet.

3. A three-dimensional temperature and velocity calculation is needed also for determining the temperature at the ice bottom, which influences the onset of basal sliding. Since the bottom temperature also depends on the geothermal heat flux, which is only poorly known, the temperature distribution within the bedrock has to be calculated too, especially in transient situations.

4. Some form of (temperature dependent) basal sliding has to be added. The omission of sliding probably accounts for the areas of negative mass balance of Fig. 9. In these regions, the bottom temperature is also at the pressure melting point.

References

Budd, W.F., et al., 1971: Derived physical charcteristics of the Antarctic-Ice-Sheet. Mark I, Melbourne, University of Melbourne, Meteorology Dept., Publication No. 18

Budd, W.F., P.L. Keage, and N.A. Blundy, 1979: Empirical studies of ice sliding. Journal of Glaciology 23: 157-170

CLIMAP, 1976: The surface of the ice-age earth. Science 191, 1131-1136

Drewry, D.J. (ed.), 1983: Antarctica in glaciological and geophysical folio. Scott Polar Research Institute Cambridge

Hutter, K., 1983: Theoretical Glaciology. Reidel Publishing Company, Dordrecht

Jenssen, D., 1977: A three-dimensional polar ice-sheet model. Journal of Glaciology 18, 373-389

MacAyeal, D.R., and R.H. Thomas, 1980: Ice-shelf grounding: ice and bedrock temperature changes. Journal of Glaciology 25, 397-400

MacAyeal, D.R., and R.H. Thomas, 1982: Numerical modeling of ice-shelf motion, Annals of Glaciology 3, 189-194

Mahaffy, M.W., 1976: A three dimensional numerical model of ice-sheets: Test on the Barnes-Ice-Cap, Northwest Territories. Journal of Geophysical Research 81, 1059-1066

Oerlemans, J., 1982: A model of the Antarctic-Ice-Sheet. Nature 297, 550-553

Oerlemans, J., and C.J. van der Veen, 1984: Ice-Sheets and Climate. D.Reidel Publishing Company, Dordrecht

Oswald, G., K., A., and G.de Q. Robin, 1973: Lakes beneath the Antarctic-Ice-Sheet. Nature 245, 251-254

Paterson, W.S.B., 1981: The physics of glaciers. Pergamon Press (2nd edition)

Weertman, J., 1976: Milankovitch solar radiation variations and ice age ice-sheet sizes. Nature, 261, 17-20

Saltzman, B., 1984: On the role of equilibrium atmospheric climate models in the theory of long-period glacial variations. Journal of Atmospheric Sciences, 7-14

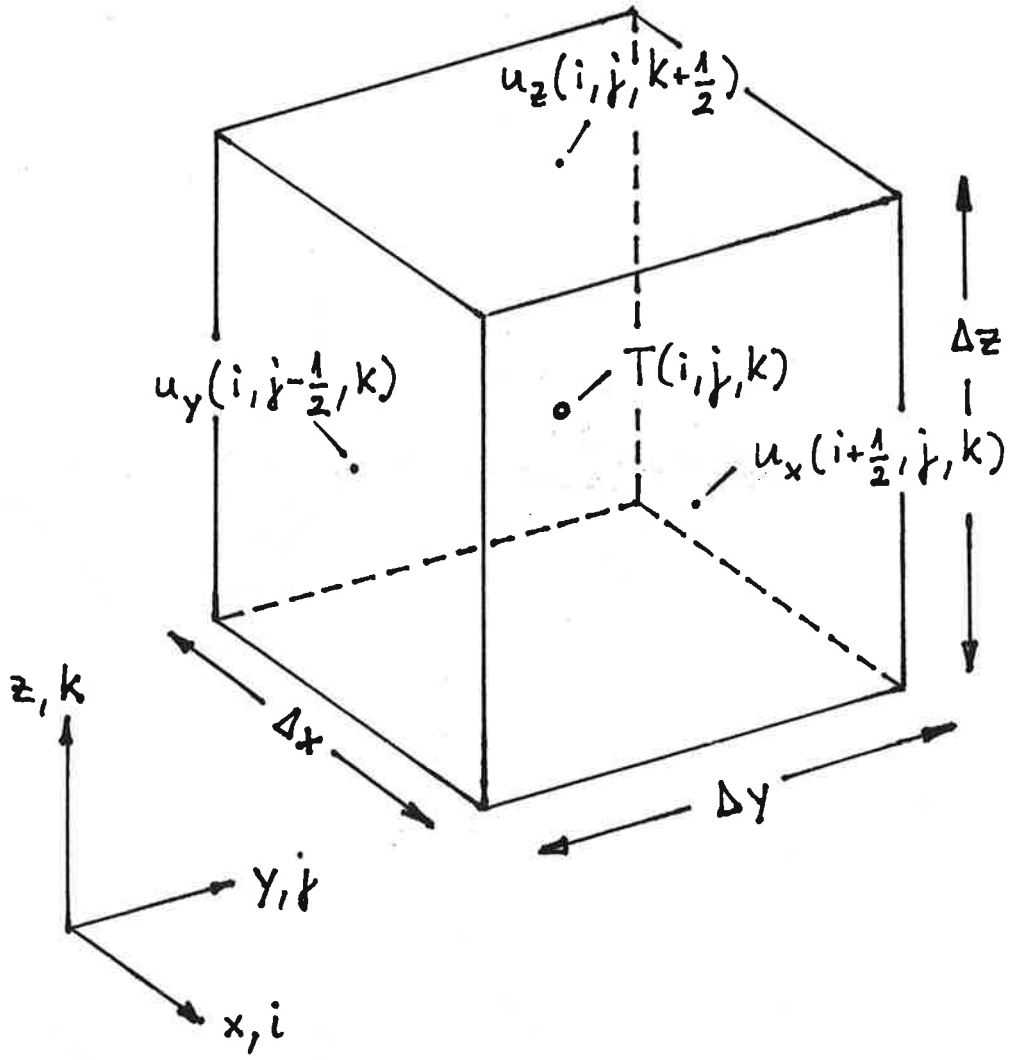

Fig. 1. Definition of the staggered grid and volume element $\Delta V = \Delta x \Delta y \Delta z$ used for numerical calculations Temperature T is defined at the center of the cube and the flow components are determined at the centers of the corresponding 6 cube surfaces.

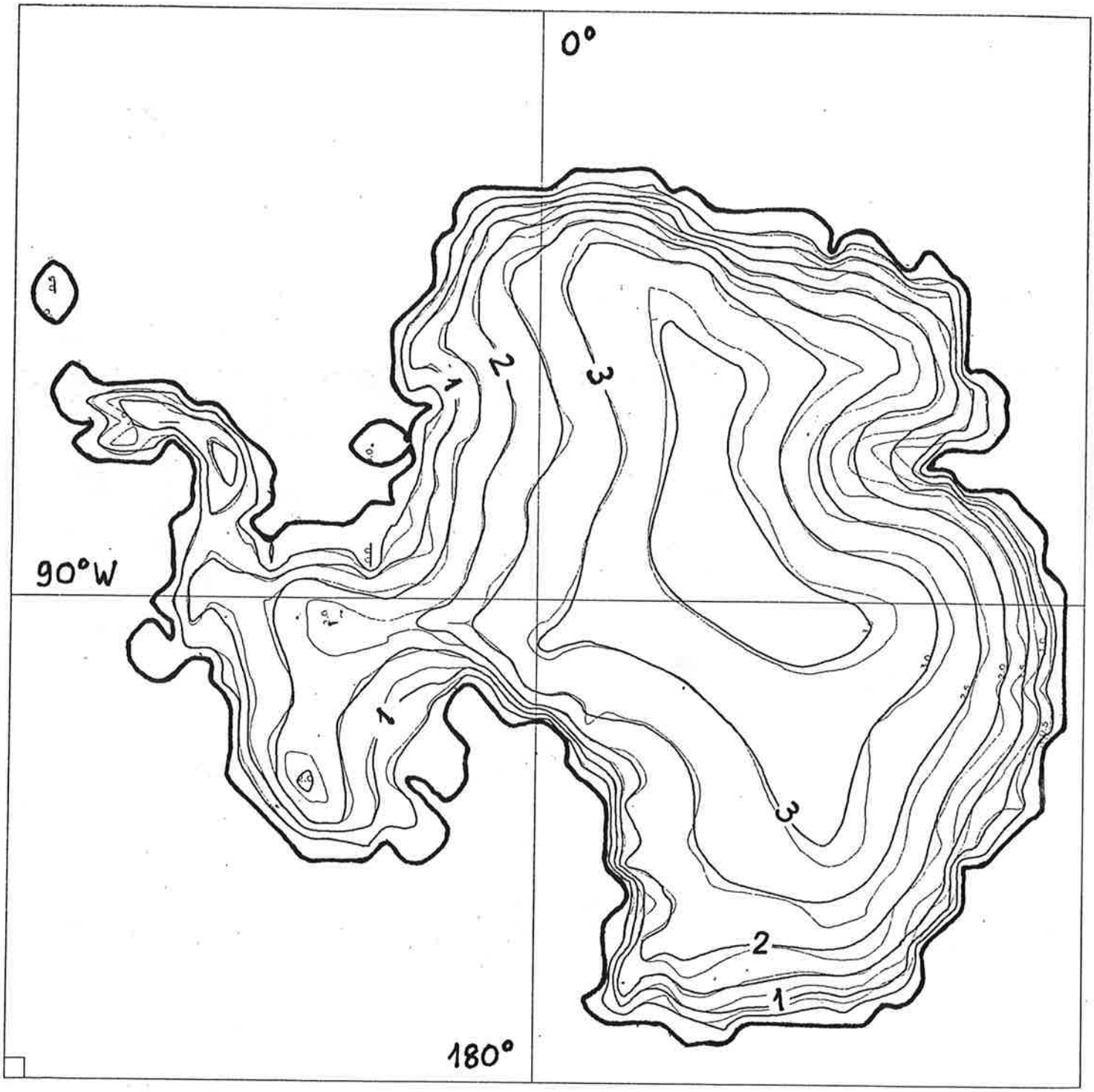

Fig. 2. Surface height (km) of the Antarctic-Ice-Sheet (thin line) taken from Drewry (1983) and after smoothing (thick line).

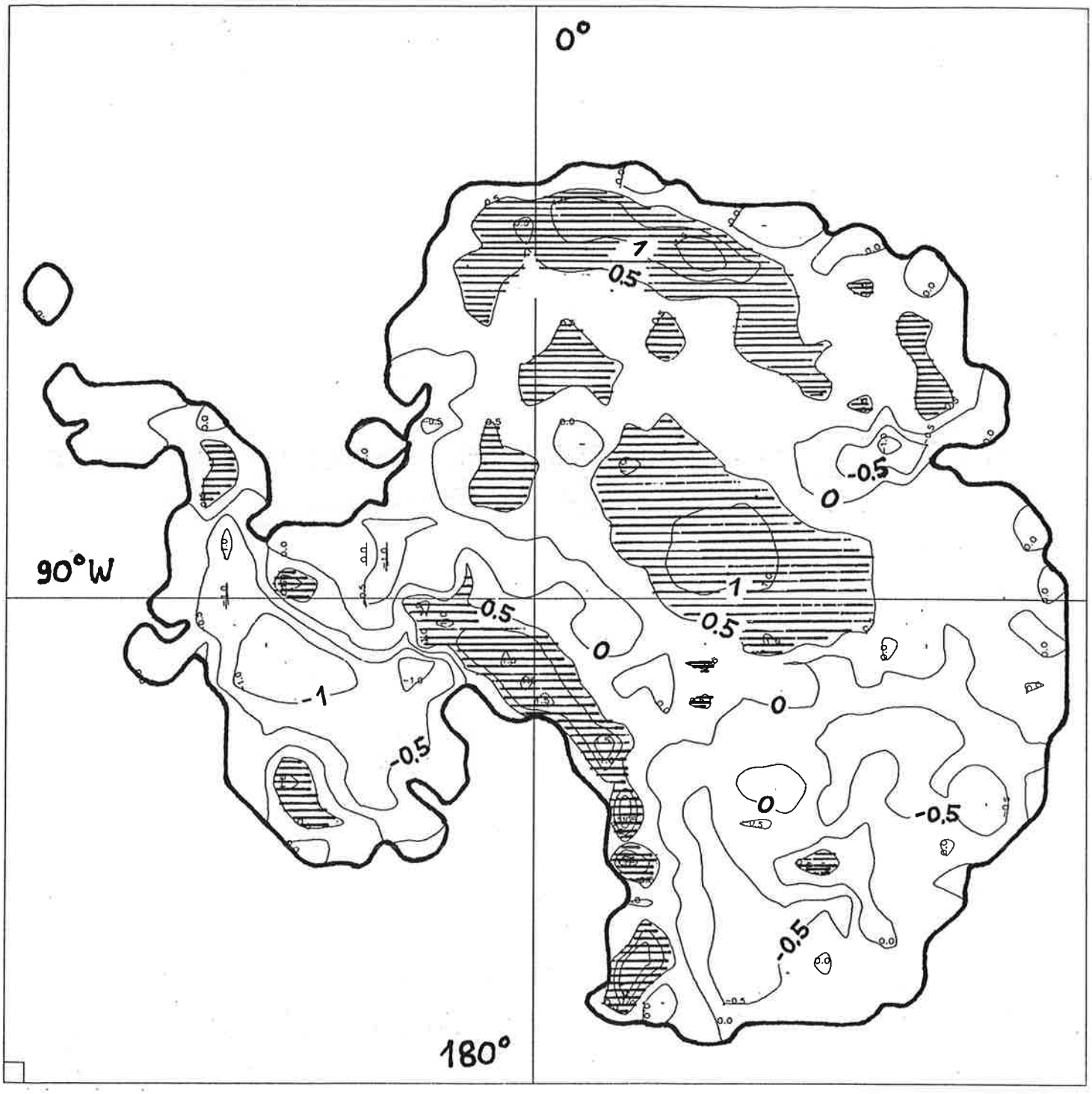

Fig. 3. Bottom height (km) of the Antarctic-Ice-Sheet. Heights above 500 m are shaded.

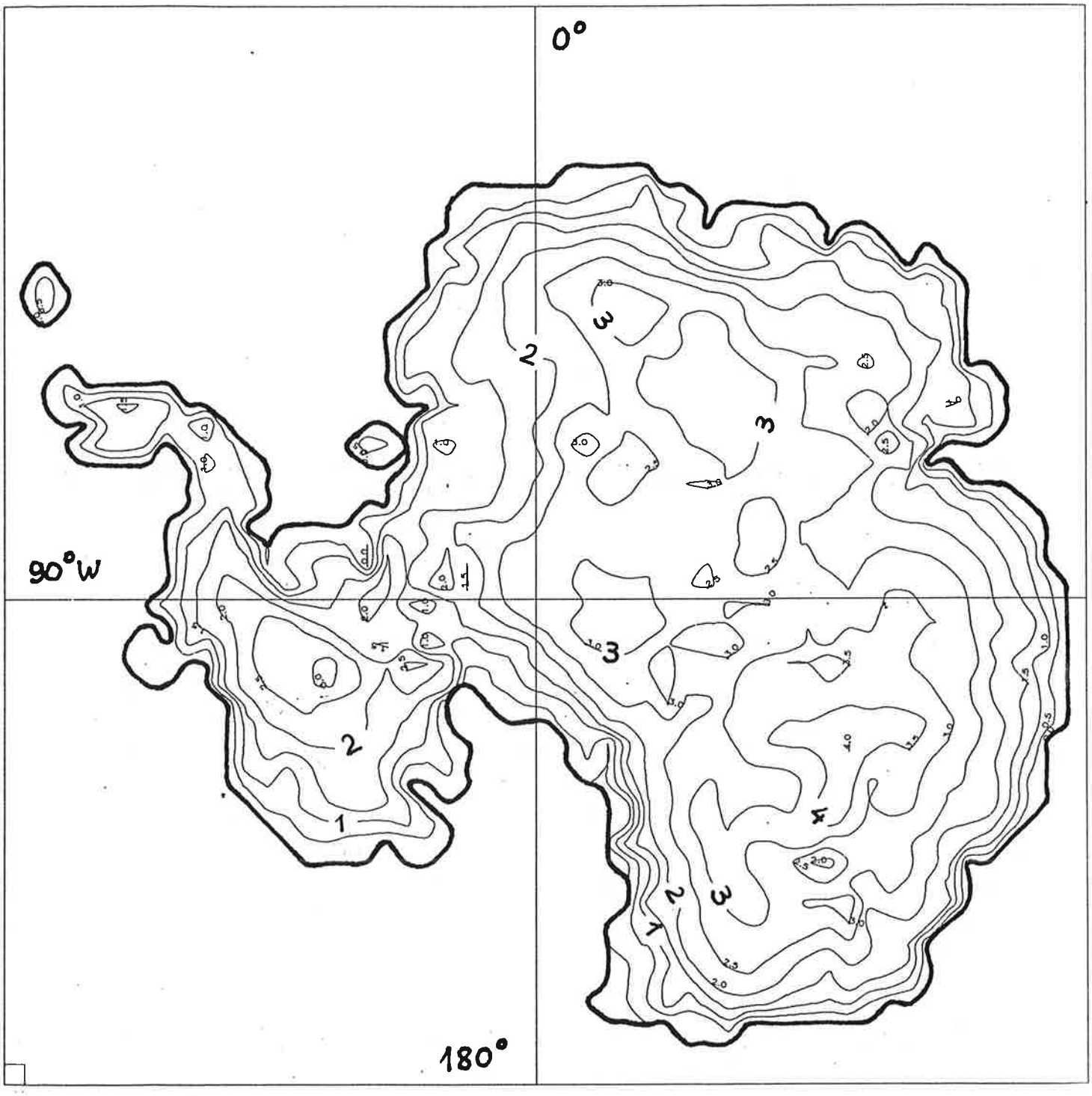

Fig. 4. Thicknesses (km) of the Antarctic-Ice-Sheet.

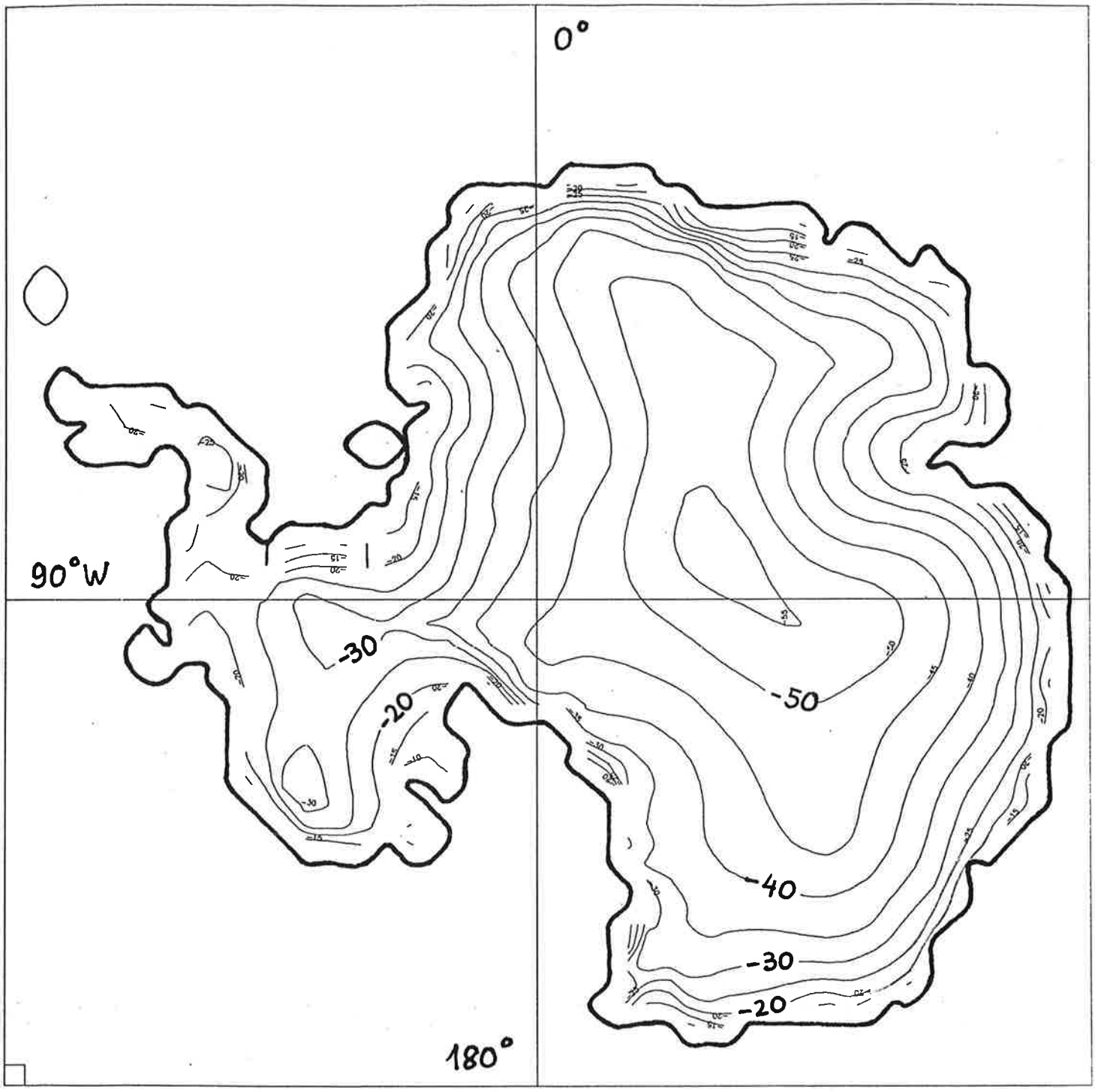

Fig. 5. Isolines of prescribed surface temperature (°C) used for calculating the interior temperature distribution.

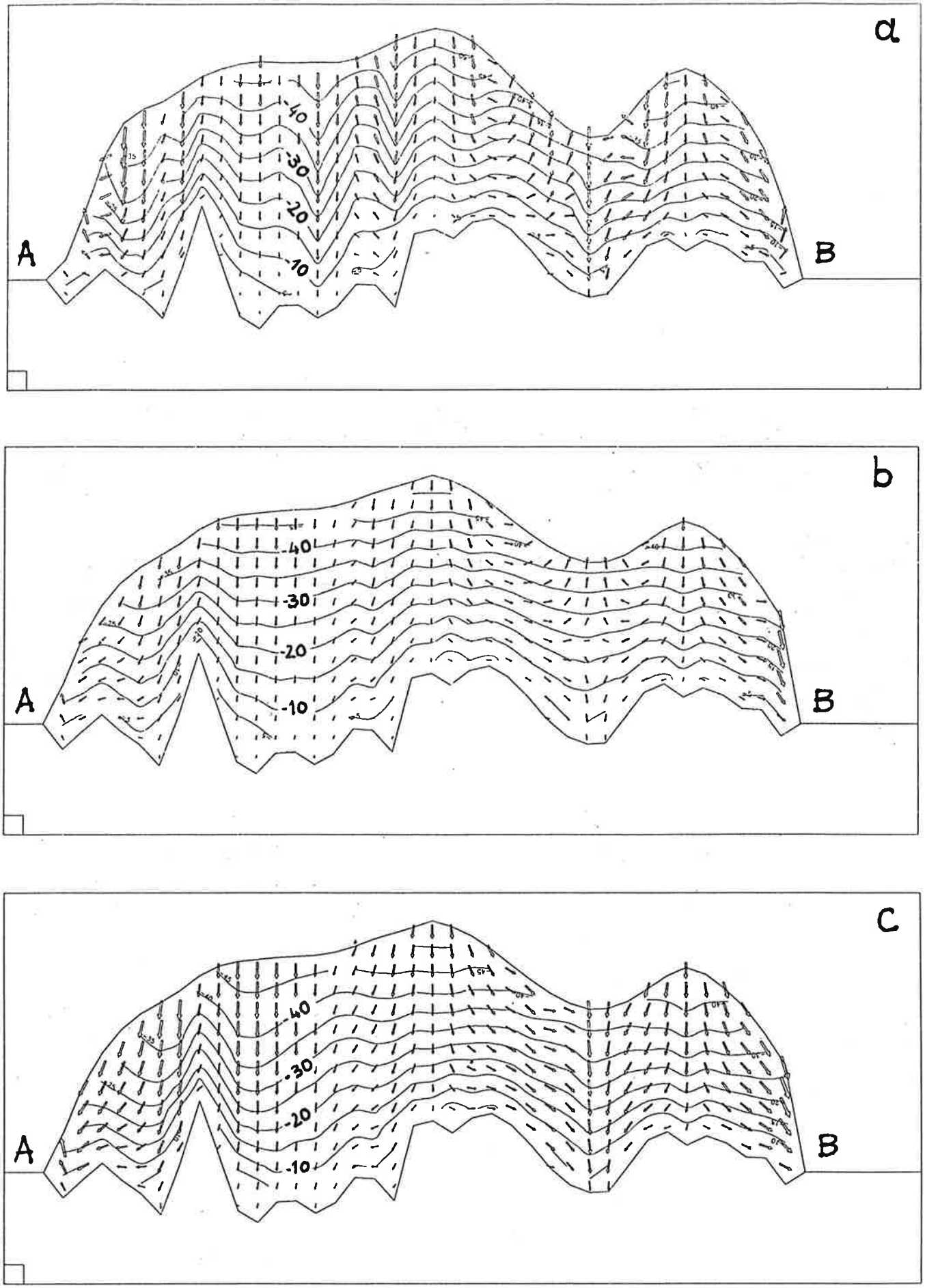

Fig. 6. Vertical profiles of velocity and temperature for different modes of calculation: a) unsmoothed surface height, velocity and temperature uncoupled; b) smoothed surface, velocity and temperature uncoupled; c) smoothed surface, velocity and temperature coupled.

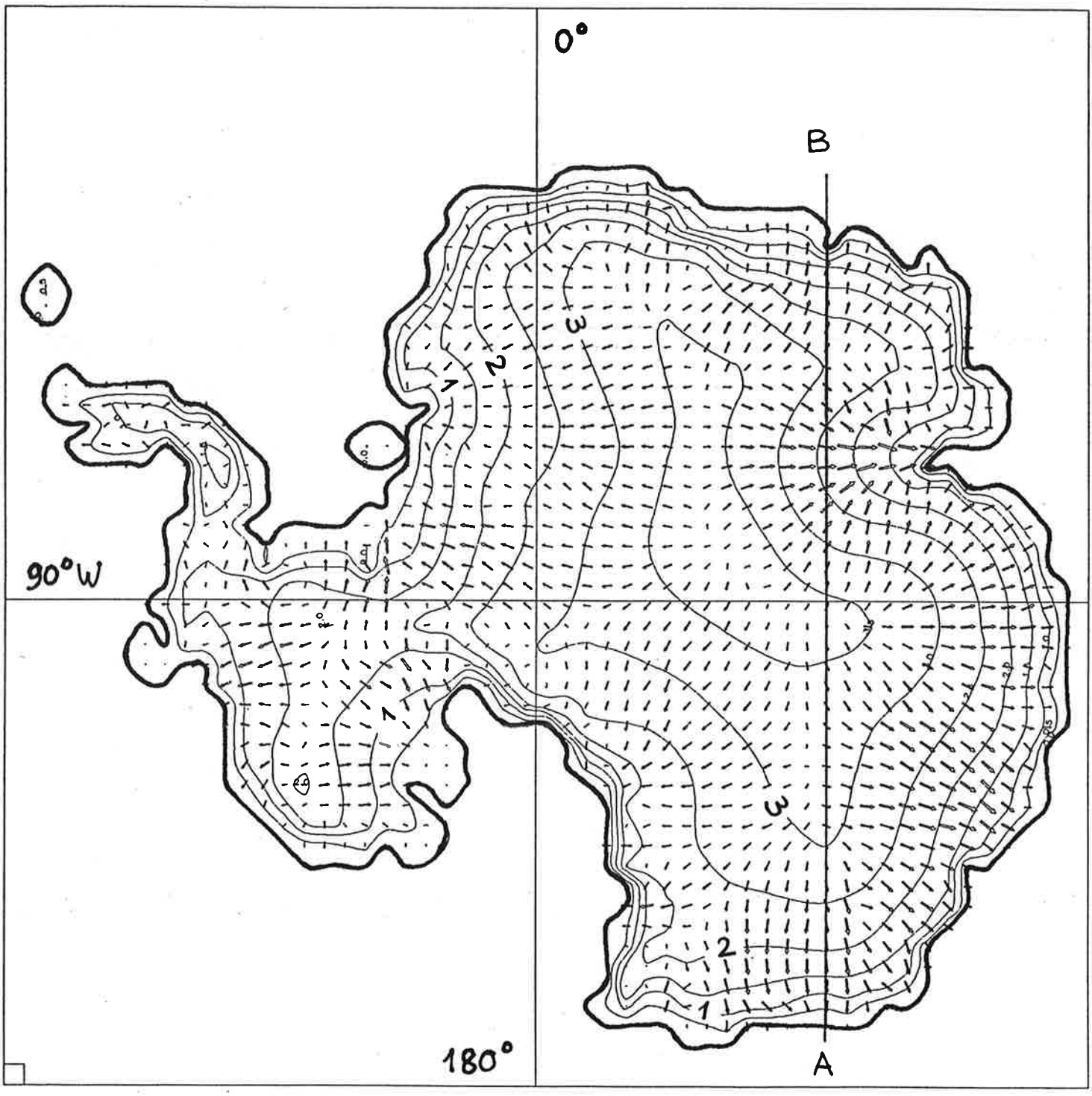

Fig. 7. Vertically integrated ice flux (arrows) and isolines of the smoothed surface height (km).

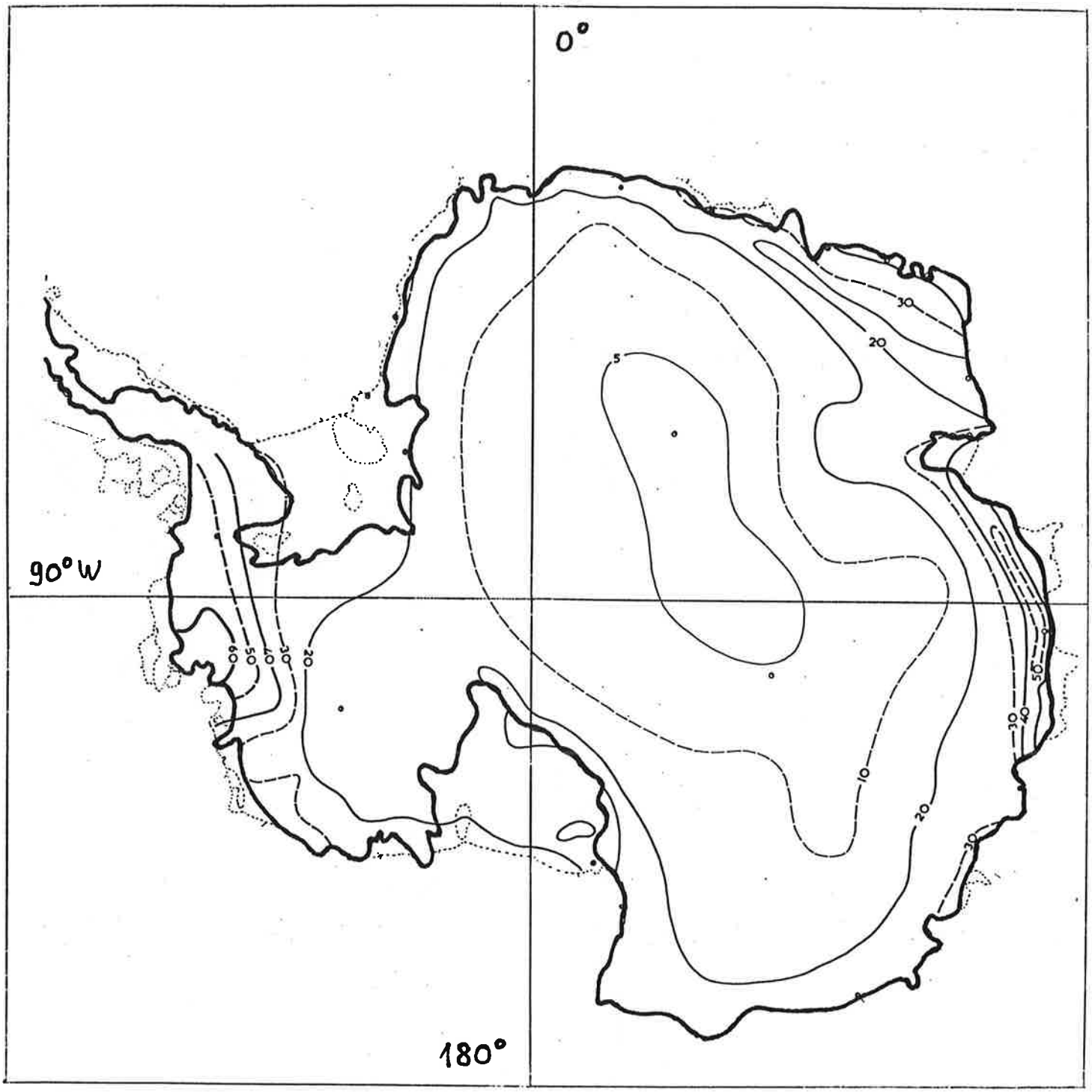

Fig. 8. Observed accumulation rates (cm a^{-1}) on the Antarctic-Ice-Sheet (after Budd et al., 1971).

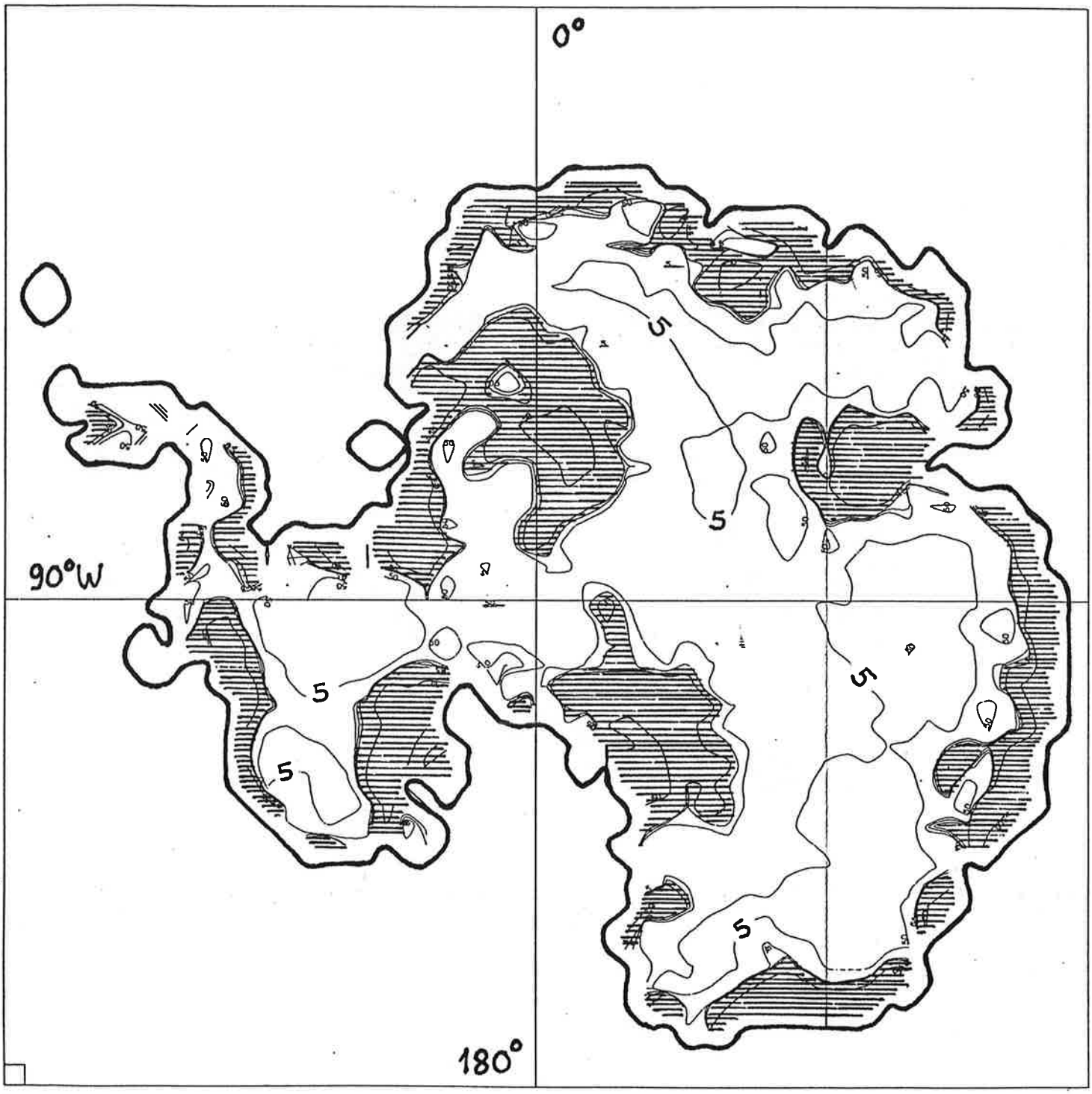

Fig. 9. Model accumulation (cm a^{-1}) to keep the (model) Antarctic-Ice-Sheet in a stationary state. Areas of negative mass balance (convergence of vertically integrated ice flux) are shaded.

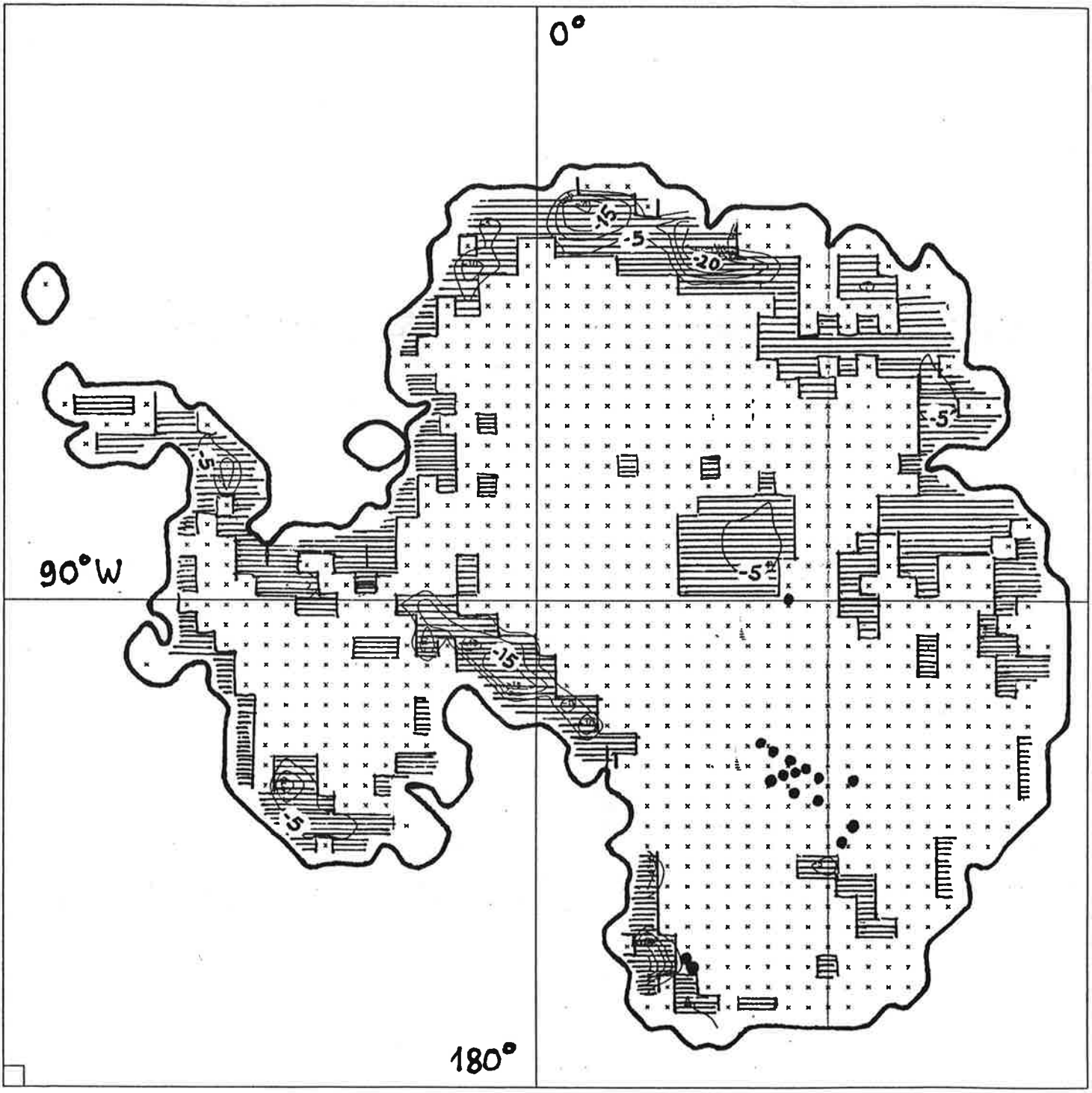

Fig. 10. Isolines of bottom temperature (°C) and locations of sub-ice lakes (dots). Areas where the ice is frozen to the bedrock are shaded.

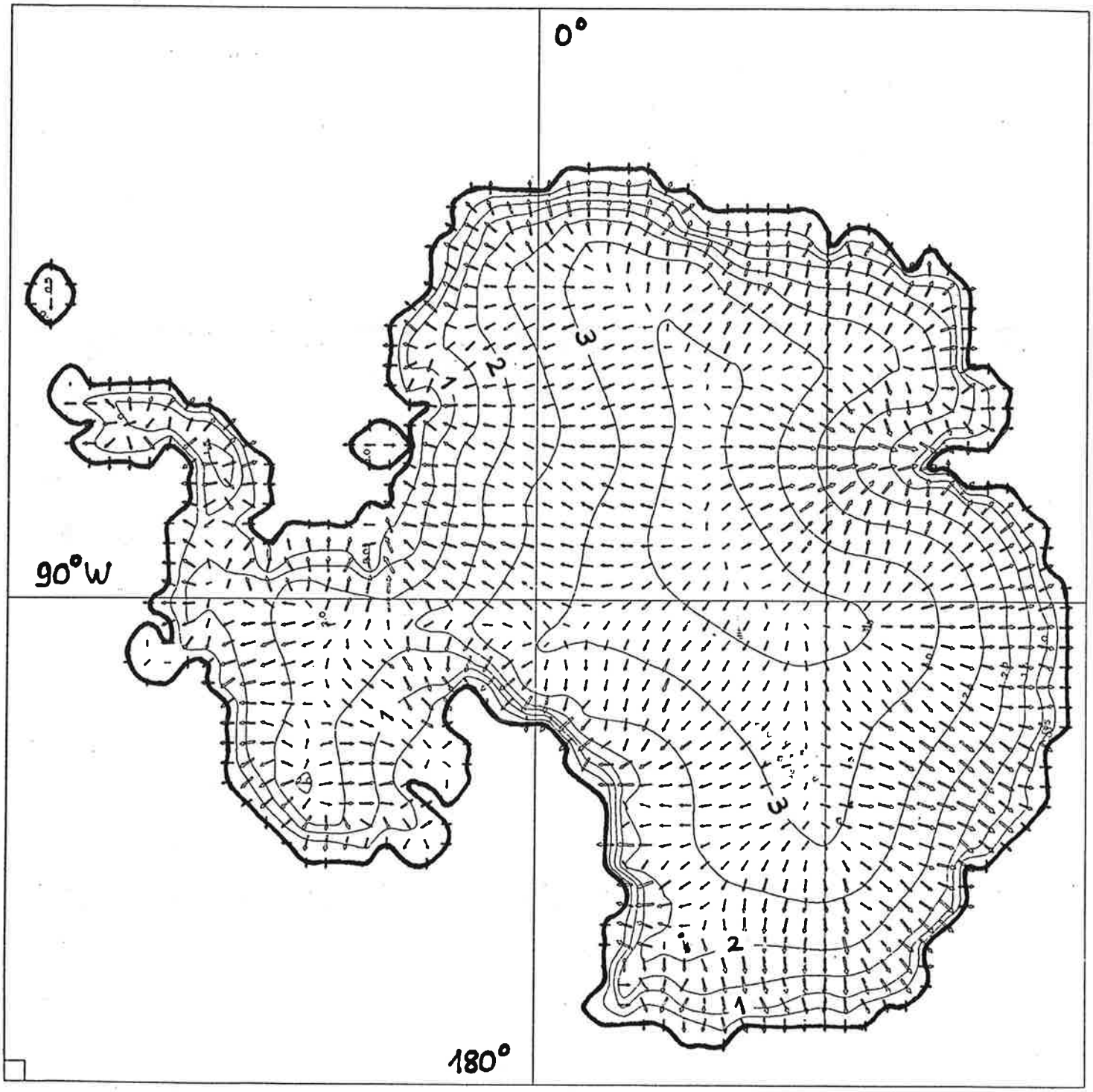

Fig. 11. Vertically integrated ice flux (arrows) and isolines of the smoothed surface height (km) for the basal sliding experiment of section 3.4.

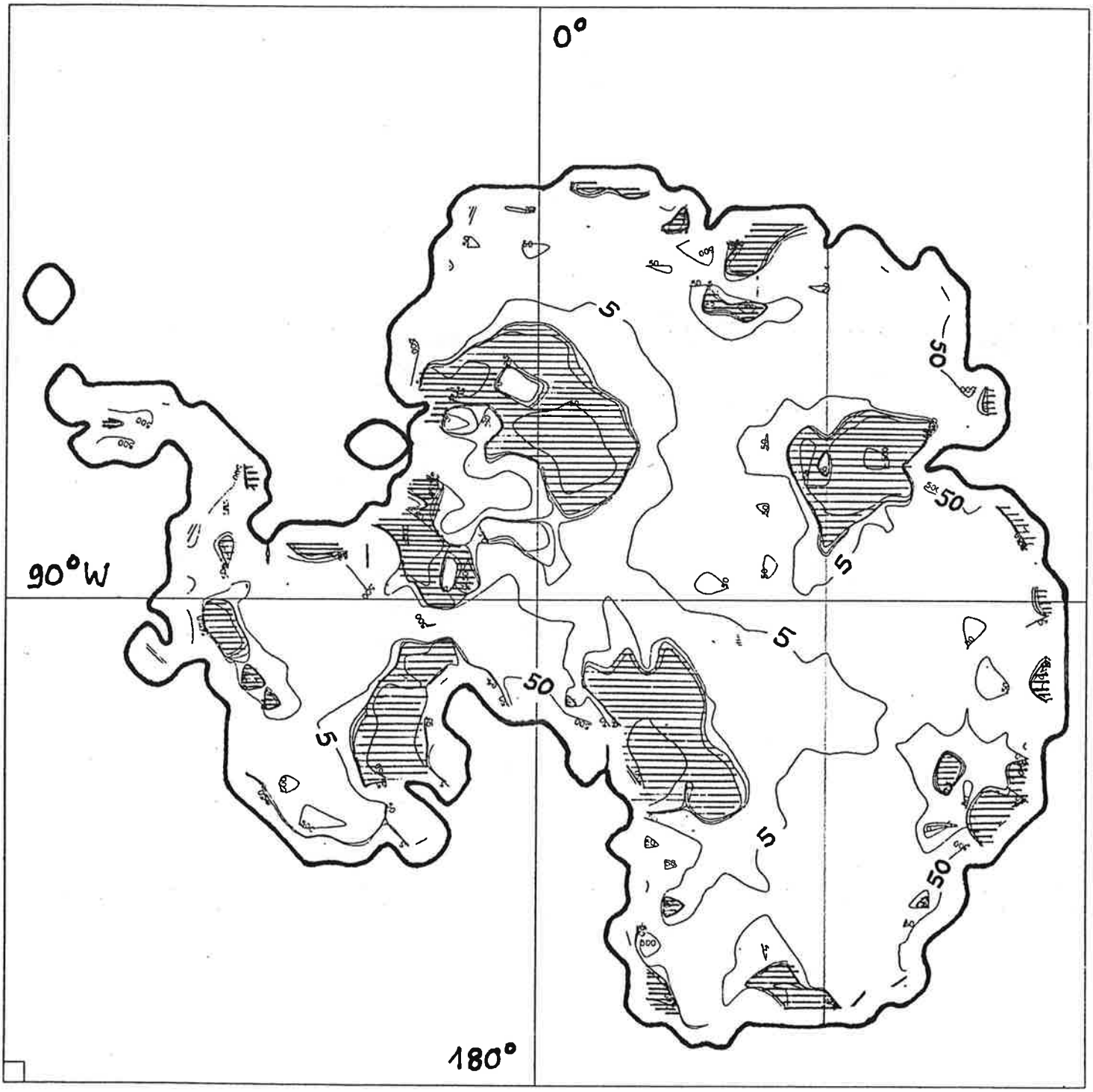

Fig. 12. Model accumulation (cm a-1) in the case of basal sliding. Areas of negative mass balance are shaded.

Fig. 12

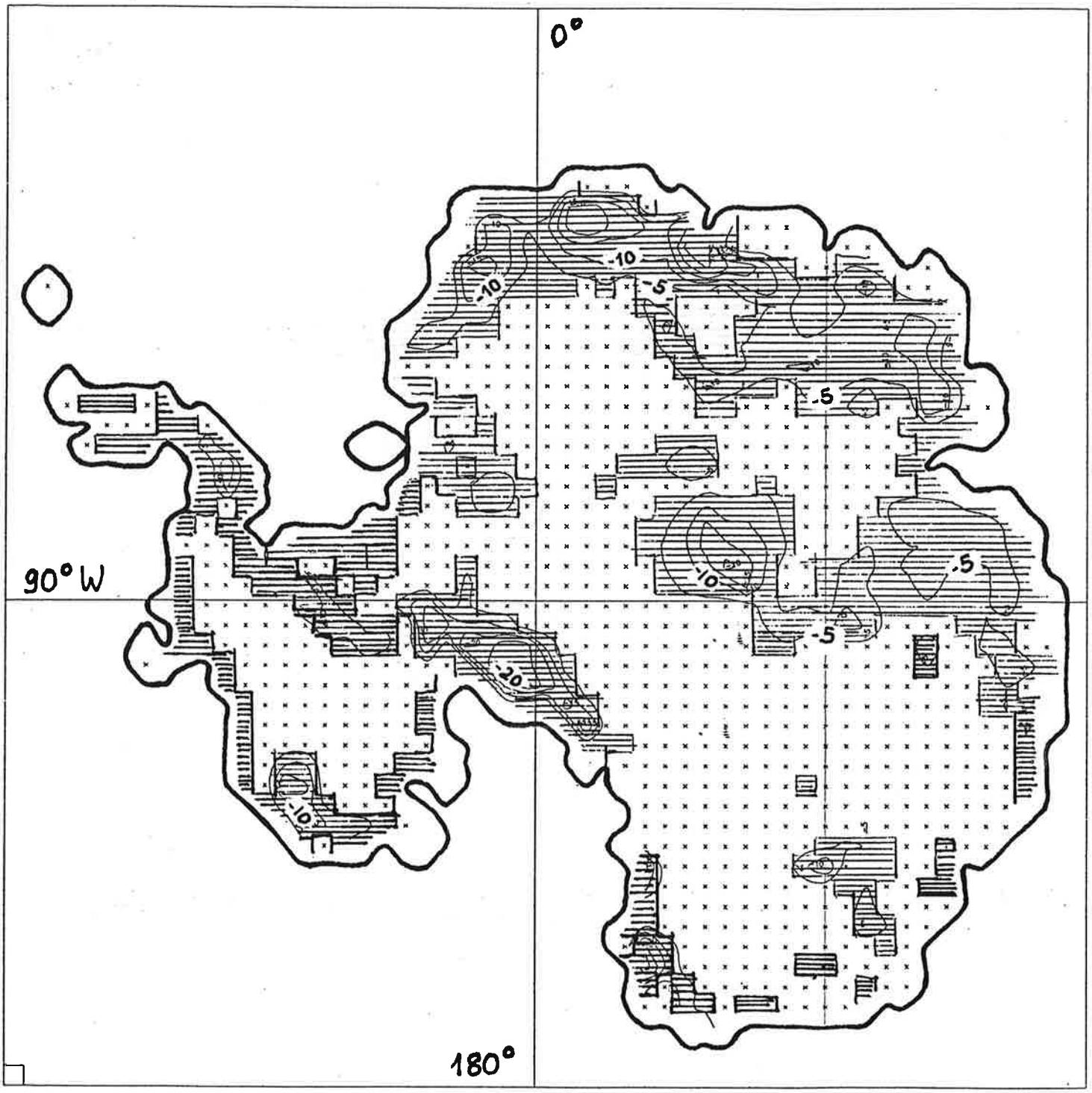

Fig. 13. Isolines of bottom temperature (°C) in the case of basal sliding. Areas where the ice is frozen to the bedrock are shaded.